A Comparison of Ni- and Pd-Diimine Complexes as Catalysts for Ethylene/Methyl Acrylate Copolymerization. A Static and Dynamic Density Functional Theory Study

Artur Michalak,*[,†,‡] and Tom Ziegler[†]

Department of Chemistry, University of Calgary, University Drive 2500, Calgary, Alberta, Canada T2N 1N4, and Department of Theoretical Chemistry, Faculty of Chemistry, Jagiellonian University, R. Ingardena 3, 30-060 Cracow, Poland

Received December 27, 2002

Gradient-corrected density functional theory (DFT) has been used to study the elementary reactions for the mechanism of ethylene/methyl acrylate copolymerization catalyzed by Pd- and Ni-diimine complexes, N∧N-M-(n-C_3H_7)$^+$; N∧N = −N(Ar)-C(R)-C(R)-N(Ar)−. The main goal was to understand the differences between the Pd- (active copolymerization catalyst) and Ni-systems (inactive under the same conditions) and, thus, the factors that determine the catalyst activity in these processes. The acrylate insertion into the metal−alkyl bond, the stability of the insertion products, and the complexation of the next monomer (ethylene and acrylate) have been studied by static calculation, and the molecular dynamics approach has been applied to study the ethylene insertion following the acrylate insertion. To account for the steric influence on the acrylate insertion barriers and the stability of isomeric chelate-ethylene complexes, calculations have been carried out for both the model [Ar = H, R = H] and the real catalyst [Ar = 2,6-C_6H_3(i-Pr)$_2$; R = CH_3]. It has been found that acrylate insertion follows the same mechanism for the Ni- and Pd-complexes. The 2,1-insertion is a preferred pathway for the acrylate incorporation. For both catalysts the acrylate 2,1-insertion barriers (12.4 and 13.5 for Pd and Ni with the real catalyst, respectively) are lower than the barriers for the insertion of ethylene (16.8 and 14.2 for Pd and Ni). The chelates formed after the acrylate insertion are slightly more stable for Ni than for Pd, with the five-membered system having the lowest energy. The MD results show that after the acrylate incorporation the activation barriers for the ethylene insertions starting from the isomers without the chelating bond are substantially lower than those starting from the chelated complexes. The ethylene insertion barriers are lower for Ni than for Pd in any case. The barriers for the opening of the chelate prior to insertion have been found to be lower for Pd ($\Delta G^{\ddagger}$ = 11.3 kcal/mol) than for Ni (14.4 kcal/mol) for the generic catalyst. The opening of the chelates is facilitated by the presence of the steric bulk on the catalyst; the effect is stronger for Ni than for Pd. Therefore, the present results suggest that the most important difference in the mechanisms of the copolymerization of the methyl acrylate with ethylene between the Pd- and Ni-diimine complexes is an initial poisoning of the catalyst by the O-binding mode in the latter case.

Introduction

The development of a single-site Ziegler−Natta-type catalyst capable of copolymerizing α-olefins with monomers containing polar groups is one of the major goals in the design of new polymerization catalysts. Of special interest are the oxygen- and nitrogen-containing monomers, such as vinyl alcohols, ethers, esters, and nitriles. The progress in this field has been reviewed recently by Boffa and Novak.[1] The traditional heterogeneous Ziegler−Natta catalyst[2] and the early transition metal complexes[3] are usually poisoned by polar monomers. The late transition metal based complexes[4,5] are more promising, as they are more functional group tolerant.

† University of Calgary.
‡ Jagiellonian University.

(1) Boffa, L. S.; Novak, B. M. *Chem. Rev.* **2000**, *100*, 1479, and references therein.

(2) Ziegler, K.; Holtzkamp, E.; Martin, H.; Breil, H. *Angew. Chem.* **1955**, *67*, 541. Ziegler, K.; Holtzkamp, E..; Breil, H.; Martin, H *Angew. Chem.* **1955**, *67*, 426. Natta, G. *J. Polym. Sci.* **1955**, *16*, 143; Natta, G. *Angew. Chem.* **1956**, *68*, 393.

(3) Sinn, H.; Kaminsky, W.; Vollmer, H. J.; Woldt, R. *Angew. Chem., Int. Ed. Engl.* **1980**, *19*, 380. Sinn, H.; Kaminsky, W. *Adv. Organomet. Chem.* **1980**, *18*, 99. Wild, F. R. W. P.; Zsolnai, L.; Huttner, G.; Brintzinger, H. H. *J. Organomet. Chem.* **1982**, *232*, 233. Kaminsky, W.; Kulper, K.; Brintzinger, H. H.; Wild, F. R. W. P. *Angew. Chem., Int. Ed. Engl.* **1985**, *24*, 507. Togni, A.; Halterman, R. L. *Metallocenes*; Wiley: Weinheim, 1998. Brintzinger, H. H.; Fischer, D.; Mülhaupt, R.; Rieger, B.; Waymouth, R. M. *Angew. Chem., Int. Ed. Engl.* **1995**, *34*, 1143, and references therein. McKnight, A. L.; Waymouth, R. M. *Chem. Rev.* **1998**, *98*, 2587, and references therein. Alt, H. G.; Koppl, A. *Chem. Rev.* **2000**, *100*, 1205, and references therein. Coates, G. W. *Chem. Rev.* **2000**, *100*, 1223, and references therein. Resconi, L.; Cavallo, L.; Fait, A.; Piemontesi, F. *Chem. Rev.* **2000**, *100*, 1253, and references therein. Marks, T. J., Stevens, J. C., Eds. *Topics in Catalysis*; Baltzer: Amsterdam, 1999; Vol. 7, and references therein.

(4) Britovsek, G. J. P.; Gibson, V. C.; Wass, D. F. *Angew. Chem., Int. Ed.* **1999**, *38*, 428, and references therein.

(5) Ittel, S. D.; Johnson, L. K.; Brookhart, M. *Chem. Rev.* **2000**, *100*, 1169, and references therein.

10.1021/om021044e CCC: $25.00
Publication on Web 05/21/2003

The first successful example is the Brookhart Pd-diimine catalyst,[5,6] capable of copolymerizing ethylene with acrylates.[7,8] Interestingly, the analogous Ni-based catalyst, although effective in α-olefin homopolymerization, is not active in polar copolymerization under the same reaction conditions. To date little in terms of mechanistic studies is available to explain this difference between the nickel and palladium systems.

The major goal of this investigation is to perform a comparative study on the ethylene/acrylate copolymerization catalyzed by either Ni- or Pd-diimine complexes. The mechanistic aspects of the polymerization processes catalyzed by the diimine catalysts have been studied extensively by experimental[5,8−11] and theoretical methods.[12−23] As far as the polar copolymerization is concerned, we have previously reported[19] the computational studies on the polar monomer binding mode to Ni- and Pd-catalysts with the diimine and salicylaldiminato ligands; similar studies were performed for the nitrogen-containing monomers.[22] Binding and migratory insertion of various olefinic monomers was studied by DFT calculations for the Pd-diimine catalyst by Schenck et al.[14] Previously,[20] we have presented results from static DFT studies on the elementary steps in the ethylene-acrylate copolymerization catalyzed by Pd-diimine systems. Very recently similar computational investigations performed for Pd-catalyzed copolymerization of ethylene with methyl acrylate and other polar monomers have been reported by Philipp et al.[23] However, the elementary reactions of the polar copolymerization processes with the Ni-diimine complexes have not been studied yet.

The mechanism of polar copolymerization (see Scheme 1) involves competition between binding of the nonpolar and polar monomer. In the standard Coose−Arlman mechanism[24] for α-olefin polymerization the monomer insertion follows the complexation of the olefin by its double C═C bond (π-complex, **2** and **4** in Scheme 1a). The polar monomer may be bound in addition by its functional group, e.g., carbonyl oxygen in the case of acrylates (O-complex, **3**) rather than its C═C bond. The competition between the two binding modes of a polar olefin is one of the factors of importance for catalyst activity, as insertion of the polar monomer in a random copolymerization mechanism may start from the π-complex only, whereas formation of a too stable O-complex will poison the catalyst. In the case of diimine complexes, it has been found[19] that for the Ni-system the O-binding mode is preferred by ca. 3 kcal/mol, while the π-complex has the lower energy for the Pd-catalyst.

The polar monomer insertion results in the formation of chelates (**9**, **10**, **11**), more stable than the agostic complexes (γ- and β-agostic, **7** and **8** of Scheme 1a), which are typical products of the nonpolar olefin insertion. It has been found experimentally[8] and confirmed by theoretical studies[20,23] that the six-membered chelate (**11**) is a resting state for the catalyst in acrylate polymerization catalyzed by Pd-diimine complexes. Formation of the chelates is followed by the insertion of the next monomer, again starting from the corresponding π-complexes (**12**−**14** and **15**−**17** of Scheme 1b). Here as well, the polar monomer may be bound alternatively by its functional group (**18**−**20** of Scheme 1b) and potentially poison the catalyst. It has been found for the Pd-catalyst that the chelating Pd−O bond is still present in the most stable geometries of the π-complexes **12**−**20**. The next monomer insertion can potentially start from such complexes, or from higher energy isomeric systems in which the chelating ring has been opened. Such a two-step chelate opening mechanism (see Scheme 1c) seems to be preferred for the Pd-catalyst.[20]

In the following we will present the results of mechanistic studies on the Ni-diimine catalyst and compare them to the corresponding results for the Pd-systems. In the acrylate insertion, the stability of the alternative insertion products and the stability of the next monomer complexes have been studied by static DFT calculations. In addition, molecular dynamics (MD) has been employed to study important details of the chelate opening reactions in the copolymerization processes catalyzed by both Ni- and Pd-diimine systems, such as the stability of alternative ethylene π-complexes derived from the chelates, the alternative pathways for ethylene insertion, and the isomerization reaction of **14**, resulting in opening of the chelates. As we argued in a previous study,[20] there exist many isomeric structures of the π-complexes **12**−**20** and consequently many alternative transition states for the ethylene insertion. Thus, a MD approach seems to be appropriate for a study of these reactions, as it directly provides information about the complete reaction pathways and the entropic effects at finite temperatures. The results of this study will be used to draw conclusions about the factors determining the catalyst activity in the polar copolymerization processes.

Computational Details and the Model Systems

The elementary reactions of the copolymerization process and the molecular systems studied in the present work are shown in Scheme 1. The mechanistic DFT studies of the ethylene and methyl acrylate copolymerization catalyzed by Pd-diimine complexes have been reported previously.[20] Here, we performed similar static DFT calculations on the acrylate

(6) Johnson, L. K.; Killian, C. M.; Brookhart, M. *J. Am. Chem. Soc.* **1995**, *117*, 6414. Killian, C. M.; Tempel, D. J.; Johnson, L. K.; Brookhart, M. *J. Am. Chem. Soc.* **1996**, *118*, 11664.
(7) Johnson, L. K.; Mecking, S.; Brookhart, M. *J. Am. Chem. Soc.* **1996**, *118*, 267.
(8) Mecking, S.; Johnson, L. K.; Wang, L.; Brookhart, M. *J. Am. Chem. Soc.* **1998**, *120*, 888.
(9) Tempel, D. J.; Johnson, L. K.; Huff, R. L.; White, P. S.; Brookhart, M. *J. Am. Chem. Soc.* **2000**, *122*, 6686.
(10) Shultz, L. H.; Brookhart, M. *Organometallics* **2001**, *20*, 3975.
(11) Shultz, L. H.; Tempel, D. J.; Brookhart, M. *J. Am. Chem. Soc.* **2001**, *123*, 11539.
(12) Musaev, D. G.; Froese, R. D. J.; Morokuma, K. *Organometallics* **1998**, *17*, 1850.
(13) Froese, R. D. J.; Musaev, D. G.; Morokuma, K. *J. Am. Chem. Soc.* **1998**, *120*, 1581.
(14) Schenck, H.; Stromberg, S.; Zetterberg, K.; Ludwig, M.; Akermark, B.; Svensson, M. *Organometallics* **2001**, *20*, 2813.
(15) Deng, L.; Margl, P.; Ziegler, T. *J. Am. Chem. Soc.* **1997**, *119*, 1094.
(16) Deng, L.; Woo, T. K.; Cavallo, L.; Margl, P. M.; Ziegler, T. *J. Am. Chem. Soc.* **1997**, *119*, 6177.
(17) Michalak, A.; Ziegler, T. *Organometallics* **1999**, *18*, 3998.
(18) Michalak, A.; Ziegler, T. *Organometallics* **2000**, *19*, 1850.
(19) Michalak, A.; Ziegler, T. *Organometallics* **2001**, *20*, 1521.
(20) Michalak, A.; Ziegler, T. *J. Am. Chem. Soc.* **2001**, *123*, 12266.
(21) Michalak, A.; Ziegler, T. *J. Am. Chem. Soc.* **2002**, *124*, 7519.
(22) Deubel, D.; Ziegler, T. *Organometallics* **2002**, *21*, 1603.
(23) Phillip, D. M.; Muller, R. P.; Goddard, W. A.; Storer, J.; McAdon, M.; Mullis, M. *J. Am. Chem. Soc.* **2002**, *124*, 10198.
(24) Coose, P. *J. Catal.* **1964**, *3*, 80; Arlman, E. J.; Coose, P. *J. Catal.* **1964**, *3*, 99.

Scheme 1. Mechanism of Ethylene-Methyl Acrylate Copolymerization and the Complexes Studied in the Present Work

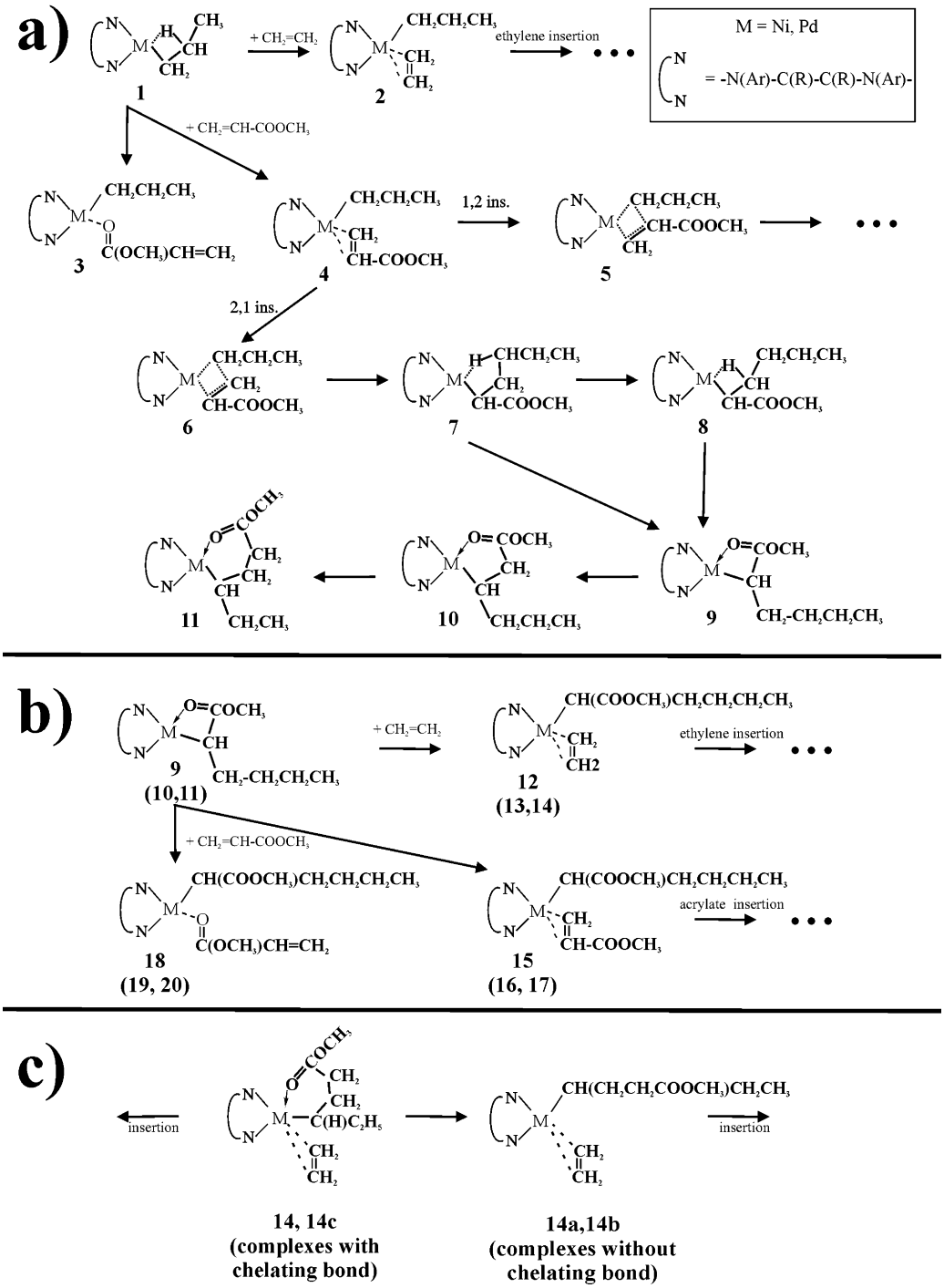

insertion process involving the Ni-diimine catalysts. In most of the calculations the diimine catalyst was modeled by a *generic* N∧N-M$^+$ complex, with M = Ni, Pd, and N∧N = −NHCHCHNH−, in which the bulky substituents of the real catalysts were replaced by hydrogen atoms. The polymer chain initially attached to the catalyst was modeled by an *n*-propyl group. The polar monomer binding modes (acrylate O- and π-complexes, **3**, and **4**) have been studied previously for both Ni- and Pd-diimine catalysts;[19] we quote these results for the sake of completeness. Starting from the acrylate π-complex **4**, both 1,2- and 2,1-acrylate insertion paths have been considered. The calculations were performed on the 1,2- and 2,1-insertion transition states (**5** and **6**, respectively). Since it was found that the 1,2-insertion TS is substantially higher in energy, further calculations have been carried out for the 2,1-insertion products only. Thus, we considered the γ- (**7**) and β-agostic complexes (**8**) and the four-, five-, and six-membered chelates (**9**, **10**, **11**) present in the 2,1-acrylate insertion path.

As the next step, formation of the ethylene (**12**, **13**, **14**) and acrylate complexes (O-binding mode: **18**, **19**, **20**, and the π-complexes **15**, **16**, **17**) resulting from the chelates has been investigated (Scheme 1b). There exist a large number of isomers for the ethylene and acrylate complexes resulting from the chelates. The structures with and without chelating metal−oxygen bonds form stable minima on the potential energy surfaces. In the case of ethylene complexes (**12**−**14**) with the Pd-catalyst we optimized geometries for 31, 20, and 21 isomers resulting from the six-, five-, and four-membered chelates, respectively. For the Ni-catalyst the geometry optimization has been performed for 10 isomers in each group,

analogous to the energetically preferred Pd-complexes. In the case of acrylate complexes resulting from the chelates (**15**−**20**) we studied only the most stable systems with the chelating bond, since the major goal of this calculations was to check the possibility of the catalyst being poisoned by formation of the O-bound complexes of acrylate. It has been found previously for the Pd-catalyst that two subsequent acrylate insertions are unlikely to happen.[20]

In addition to the structures of the generic catalyst, calculations have been performed on the *real* catalyst, with R = CH_3 and Ar = $C_6H_3(i\text{-}Pr)_2$, for the 2,1-acrylate insertion transition state **6** and the example isomers of ethylene-chelate complexes **14** in order to investigate the influence of steric bulk on the insertion barriers and the chelate opening energies. To be able to compare the results, we also performed similar DFT calculations for the ethylene π-complexes and the insertion TS with the real Ni-catalyst, since the ethylene results previously reported in the literature[12,13,15,16] involved different models (QM/MM) than the full QM (DFT) method applied for palladium.

The static DFT calculations based on the Becke−Perdew exchange−correlation functional[25] were performed using the Amsterdam Density Functional (ADF) program.[26] A standard double-ζ STO basis with one set of polarization functions was applied for H, C, N, and O atoms, while a standard triple-ζ basis set was employed for the Ni and Pd atoms.[27] The 1s electrons of C, N, O as well as the 1s−3d electrons of Pd and the 1s−2p electrons of Ni were treated as frozen core. Auxiliary s, p, d, f, and g STO functions,[26] centered on all nuclei, were used to fit the electron density and obtain accurate Coulomb and exchange potentials in each SCF cycle. The reported energy differences include first-order scalar relativistic corrections,[28] since it has been shown that such a relativistic approach is sufficient for 4d transition metal atoms.[29]

The Car−Parinello molecular dynamics (MD) approach[30] has been used to study the chelate opening reactions for both Ni- and Pd-catalysts. First, free (unconstrained) dynamics simulations have been performed for examples of the ethylene complexes resulting from the six-membered chelates (**14a**, **14b**). The purpose of this calculation was to check the stability of the higher energy complexes (without the chelating bond) on the nonzero-temperature free energy surfaces.

The ethylene insertion starting from **12**, **13**, and **14** has been studied as well by MD (Scheme 1c). As we have already mentioned, there exist a large number of isomers for the systems **12**, **13**, and **14**. Potentially, each of them can give rise to ethylene insertion. Thus, there exist a large number of ethylene insertion transition states connecting the alternative reactants on the potential energy surfaces. Therefore, the MD approach seems to be the most appropriate here, since the MD simulation provides information about the whole reaction pathway at a finite temperature, and not just about a few stationary points on the zero-temperature potential energy surfaces. Consequently, the activation free energies are available from the MD approach. Thus, the MD simulations have been carried out for ethylene insertion starting from the most stable isomers of **12**, **13**, and **14** with the Ni- and Pd-catalysts. Since we discovered the insertions from the most stable ethylene-chelate complexes have very high barriers, simulations were also carried out on the insertion starting from the examples of the higher energy isomers of **14** (with and without the chelating bond; for the Pd-catalyst). Finally, the chelate opening prior to the ethylene insertion (isomerization of the ethylene π-complexes **14**) has also been studied by the slow-growth MD simulations.

The unconstrained MD simulations for representative isomers of **14** without chelating bond were carried out at T = 300 K and T = 1300 K. Each of those simulations was performed for 20 000 time steps. For the ethylene insertion each of the slow-growth simulations (T = 300K) was performed for 20 000 time steps. The distance between the ethylene carbon atom and the alkyl α-carbon was used as the reaction coordinate, changing in the course of simulation between the values corresponding to the reactant (π-complex) and product (alkyl complex). For the slow-growth simulations modeling of the chelate opening, the distance between the metal and the carbonyl oxygen was used as a reaction coordinate, changing from the value characterizing the reactant (ethylene-chelate π-complex) to the arbitrarily chosen value of 8 bohr (sufficient to be sure that the chelating bond has been broken). Each chelate-opening simulation was performed for 30 000 time steps.

All reported MD results were obtained with the Car−Parrinello projector augmented wave (PAW) code developed by Blöchl.[31] The wave function was expanded in plane waves up to an energy cutoff of 30 Ry. The frozen core approximation has been employed; a Ne core has been used for Ni, an Ar core for Pd, and a He core for the first-row elements. Periodic boundary conditions were used, with a unit cell spanned by the lattice vectors ([0 9.5 9.5] [9.5 0 9.5] [9.5 9.5 0]) (Å). All the simulations were performed using the local density approximation in the parametrization of Perdew and Zunger[32] with gradient corrections due to Becke and Perdew.[25] To prevent electrostatic interactions between neighboring unit cells, the charge isolation scheme of Blöchl was used. Prior to the MD simulations, the molecular geometries were optimized. To achieve an evenly distributed thermal excitation, the nuclei were brought to a target temperature of 300 K (1300 K) by applying a sequence of 30 (130) sinusoidal pulses, each of which was chosen to raise the temperature by 10 K. Each of the excitation vectors was chosen to be orthogonal to the already excited modes. The warmed-up systems were equilibrated for 10 000 time steps. A time step of 7 au was used for all simulations. Constraints were maintained by the SHAKE algorithm.[33] The temperature was controlled by a Nosé thermostat.[34] The fictitious kinetic energy of the electrons was controlled in a similar fashion by a Nosé thermostat.[35] The free energy activation barriers, $\Delta G^{\ddagger}$, have been calculated from the slow-growth MD simulations with the thermodynamic integration method, by integrating the force on the constraint along the trajectory. The activation energies, $\Delta E^{\ddagger}$, were obtained from the running averages of the potential energy (with an averaging window of 200 steps). For each slow-growth simulation the TS region has been identified as the region

(25) Becke, A. *Phys. Rev. A* **1988**, *38*, 3098. Perdew, J. P. *Phys. Rev. B* **1986**, *34*, 7406. Perdew, J. P. *Phys. Rev. B* **1986**, *33*, 8822.

(26) TeVelde, G.; Bickelhaupt, F. M.; Baerends, E. J.; Fonseca Guerra, C.; Van Gisbergen, S. J. A.; Snijders, J. G.; Ziegler, T. *J. Comput. Chem.* **2001**, *22*, 931, and references therein. Baerends, E. J.; Ellis, D. E.; Ros, P. *Chem. Phys.* **1973**, *2*, 41. Boerrigter, P. M.; te Velde, G.; Baerends, E. J. *Int. J. Quantum Chem.* **1988**, *33*, 87. Versluis, L.; Ziegler, T. *J. Chem. Phys.* **1988**, *88*, 322. te Velde, G.; Baerends, E. J. *J. Comput. Phys.* **1992**, *99*, 84. Fonesca Geurra, C.; Visser, O.; Snijders, J. G.; te Velde, G.; Baerends, E. J. In *Methods and Techniques in Computational Chemistry METACC-95*; Clementi, E., Corongiu, G., Eds.; STEF: Cagliari, 1995.

(27) Snijders, J. G.; Baerends, E. J.; Vernoijs, P. *At. Nucl. Data Tables* **1982**, *26*, 483.

(28) Ziegler, T.; Tschinke, V.; Baerends, E. J.; Snijders, J. G.; Ravenek, W. *J. Phys. Chem.* **1989**, *93*, 3050. Snijders, J. G.; Baerends, E. J. *Mol. Phys.* **1978**, *36*, 1789. Snijders, J. G.; Baerends, E. J.; Ros, P. *Mol. Phys.* **1979**, *38*, 1909.

(29) Deng, L.; Ziegler, T.; Woo, T. K.; Margl, P.; Fan, T. *Organometallics* **1998**, *17*, 3240.

(30) Car, R.; Parrinello, M. *Phys. Rev. Lett.* **1985**, *55*, 2471.

(31) Blöchl, P. E. *Phys. Rev. B* **1994**, *50*, 17953. Blöchl, P. E. *J. Phys. Chem.* **1995**, *99*, 7422. Blöchl, P. E.; Senn, H. M.; Togni, A. In *Transition State Modeling for Catalysis;* ACS Symposium Series 721, Truhlar, D. G., Morokuma, K. Eds.; American Chemical Society: Washington, DC, 1998; pp 88−99.

(32) Perdew, J. P.; Zunger, A. *Phys. Rev. B* **1981**, *23*, 5048.

(33) Ryckaert, J. P.; Ciccotti, G.; Berendsen, H. J. C. *J. Comput. Phys.* **1977**, *23*, 327.

(34) Nose, S. *Mol. Phys.* **1986**, *57*, 187. Hoover, W. G. *Phys. Rev. A* **1985**, *31*, 1695.

(35) Blöchl, P. E.; Parinello, M.. *Phys. Rev. B* **1992**, *45*, 9413.

Table 1. Relative Energies[a] for the Stationary Points in the 2,1-Acrylate Insertion into the M−Alkyl Bond [M = Ni, Pd] (see Scheme 1)

structure		relative energy[a] Ni	relative energy[a] Pd[b,c]
O-complex	**3**	−21.10 (−3.97) [−13.09 (−2.99)]	−17.10 (+3.60)[b] [−10.64 (+2.96)]
π-complex	**4**	−17.10 (0.00) [−10.10 (0.00)]	−20.70 (0.00) [−13.60 (0.00)][b]
1,2-insertion TS	**5**	−0.06 (+17.06) [+4.57 (+14.67)]	+3.24 (+23.93)[c] −0.65 (+12.95)
2,1-insertion TS	**6**	−4.86 (+12.26) [+3.42 (+13.52)]	−1.31 (+19.39) [−1.16 (+12.44)][c]
γ-agostic	**7**	−21.36 (−4.23)	−19.77 (+0.93)[c]
β-agostic	**8**	−26.31 (−9.18)	−25.39 (−4.69)[c]
four-membered chelate	**9**	−36.56 (−19.43)	−33.64 (−12.95)[c]
five-membered chelate	**10**	−43.53 (−26.40)	−39.68 (−18.98)[c]
six-membered chelate	**11**	−42.59 (−25.47)	−40.77 (−20.07)[c]

[a] With respect to the isolated reactants (methyl acrylate + β-agostic alkyl complex) and to the acrylate π-complex (in parentheses), in kcal/mol. The numbers in square brackets refer to the real catalyst [R = CH_3, Ar = $C_6H_3(i\text{-}Pr)_2$]. [b] Ref 19. [c] Ref 20.

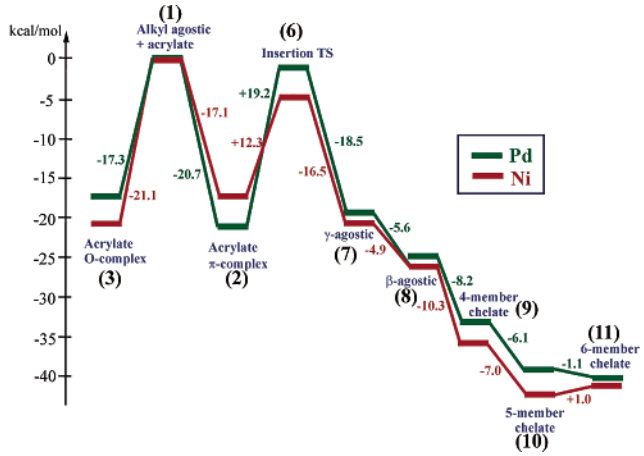

Figure 1. Energy profile for the 2,1-pathway of methyl acrylate insertion into the M−alkyl bond (M = Ni, Pd) calculated for the generic catalyst. The structure labeling (in parantheses) refers to that of Scheme 1.

around the constraint value for which (i) the force on the constraint changes sign; (ii) the maximum free energy is observed; (iii) the maximum average potential energy is observed.

Results and Discussion

Insertion of Methyl Acrylate. Table 1 lists the relative energies of the reaction intermediates present in the preferred pathway of the methyl acrylate insertion into the Ni−alkyl and Pd−alkyl bonds. The energy profiles for the methyl acrylate insertion are compared for the Ni- and Pd-catalyst in Figure 1. In the following we will discuss the methyl acrylate binding modes, the insertion transition states, and the stability of the insertion products.

As it has been mentioned already, the first step in the copolymerization mechanism involves a competition between the complexation of the polar and nonpolar olefin, and in the former case a competition between the two binding modes. The polar monomer insertion can start only from a π-complex, **4**, while the O-bound complex **3** poisons the catalyst. This has been discussed in detail in a previous study.[19] Here we will only recall for the sake of completeness that there is an important difference between the Ni- and Pd-complexes. For the Pd system, active in the polar copolymerization, the π-complex is preferred by 3.6 (generic catalyst) and 3.0 kcal/mol (real catalyst), while for the Ni-catalyst the O-complexes have lower energy by 4.0 (generic catalyst) and 3 kcal/mol (real catalyst). Thus, the Ni-catalyst is initially poisoned by formation of the "inactive" O-complex, while this is not the case for the Pd-complexes.[36]

The TS geometries have been optimized for the generic catalyst for both the 1,2- and 2,1-methyl acrylate insertions. The results show that in the case of the Ni-catalyst the 2,1-insertion is preferred by 4.8 kcal/mol. Thus, the energy difference between the two insertion TS is close, and even slightly larger than that recently reported for the Pd-catalyst (4.5 kcal/mol).[20] The steric effect on the insertion regioselectivity was discussed previously in detail for propylene[18] and acrylate;[20] for the Ni-catalyst the effect is of similar origin. It has been shown previously for the Pd-systems[20] that the relatively large preference of the 2,1-insertion cannot be overridden by steric factors in the real catalyst case. Therefore, it can be expected that the 2,1-insertion pathway is also preferred for the real Ni-catalyst. Indeed, the results of the DFT calculations for the real Ni-systems show that the 1,2-insertion TS is higher in energy by 1.2 kcal/mol than the 2,1-TS. Thus, in the following we have not studied the products of the 1,2-insertion.

The 2,1-acrylate insertion barrier for the generic Ni-catalyst (12.2 kcal/mol) is substantially lower than for the Pd-analogue (19.2 kcal/mol). However, for the real catalyst the barriers are relatively close for both systems: 12.4 kcal/mol for the Pd-complex and 13.5 kcal/mol for the Ni-complex. For comparison, we have optimized the geometry for the ethylene insertion TS with the real Ni-catalyst. The ethylene insertion barrier is 14.2 kcal/mol for the Ni-catalyst, while for the analogue Pd-catalyst it is 16.7 kcal/mol. Thus, these results clearly show that it is not the acrylate insertion that makes the copolymerization difficult in the Ni case, as for both catalysts the acrylate inserion is easier than the insertion of ethylene.

The stability of the insertion products is also quite similar for both catalysts. As for the Pd-system, the kinetic insertion product is a complex with a γ-agostic interaction, **7**, that can isomerize to the more stable β-agostic complex, **8**, or can directly form the structure involving the chelating Ni−O bond, **9**. The four-membered chelate, **9**, is more stable than the γ-agostic complex by 15.2 kcal/mol and is less stable than the structures with a five- and six-membered ring, **10** and **11**. We did not study the isomerization barriers for the **9** → **10** and **10** → **11** reactions, as they are not important for the further consideration in the present sudy. It may be expected that they are higher for Ni- than for the Pd-catalyst, as it is known that this is the case for the chain isomerization barriers in the ethylene homopo-

(36) It has been argued in ref 23 that our relative energies for the O-complex have a systematic error of ca. 2−3 kcal/mol. If this is true, then the difference between the two binding modes is larger for the Ni-catalyst, and the initial poisoning of the catalyst is even more important.

Table 2. Ethylene and Methyl Acrylate Complexation Energies after the Acrylate Insertion

reaction	energy[a] Ni-catalyst	energy[a] Pd-catalyst[b]
four-membered chelate:		
9 + C_2H_4 → **12**	−10.74	−10.14
9+ $C_2H_3COOCH_3$ → **15** (**18**)	−12.13 (−7.37)	−13.00
five-membered chelate:		
10 + C_2H_4 → **13**	−8.14	−7.79
10+ $C_2H_3COOCH_3$ → **16** (**19**)	−9.45 (−6.78)	−9.5
six-membered chelate:		
11 + C_2H_4 → **14**	−7.73	−9.09
11+ $C_2H_3COOCH_3$ → **17** (**20**)	−10.01 (−5.70)	−11.00

[a] In kcal/mol. [b] Ref 20.

lymerization processes (ca. 7 kcal/mol for Pd vs 12−15 for Ni), which proceed by a pathway similar to that expected for the chelate isomerization. Comparing the thermodynamic stability of isomeric chelates, there is a difference between the five- and six-membered structures for the two catalysts. Namely, for the Pd-catalyst the complex with a six-membered ring is the most stable isomer (lower by ca. 1 kcal/mol than the five-membered chelate), whereas in the Ni case, the five-membered chelate has the lowest energy (lower by ca. 1 kcal/mol than the five-membered ring). It should be emphasized, however, that all the chelates are more strongly stabilized (relative to the agostic complexes) for the Ni-catalyst than for Pd (see Table 1 and Figure 1). As in the case of the initial O-complexes, this reflects higher oxophilicity of the Ni-system.

The geometries of the acrylate insertion TS and the insertion products for the Ni-catalyst are qualitatively similar to those reported previously for the Pd-systems. Therefore, we do not display the structures here. The major difference between the structures observed for the two catalysts are certainly the interatomic distances between the metal and surrounding atoms, due to the difference in "sizes" of the two metal atoms. For example, the chelating Ni−O bonds in **9**, **10**, and **11** are shortened to 1.90−1.92 Å, compared to 2.09−2.11 Å in the Pd case.

Complexation of the Next Monomer after the Acrylate Insertion and the Chelate Opening. In Table 2 are listed the energies of the ethylene π-complexation (**9/10/11** + C_2H_4 → **12/13/14**) and acrylate π-complexation (**9/10/11** + $C_2H_3COOCH_3$ → **15/16/17**) for the Ni- and Pd-based catalysts. In addition for the Ni-systems, the O-binding mode of acrylate was considered, to check the possibility of catalyst poisoning by the complexes **18**, **19**, and **20** after the acrylate insertion.

As in the Pd case, the chelating Ni−O bond is present in the axial position in the geometries of the ethylene/acrylate complexes formed from the chelates with the Ni-catalyst (see Figure 2). The Ni−O distances are substantially shorter (2.09−2.11 Å) than the Pd−O bond length (2.2−2.5 Å). Again, this may be partially attributed to the difference in the "sizes" of the two metal atoms.

The results of Table 2 clearly indicate that there in no qualitative difference between the two catalysts as far as the energetics of the formation of the ethylene/acrylate complexes derived from the chelates is concerned. As in the Pd case, the ethylene binding energies

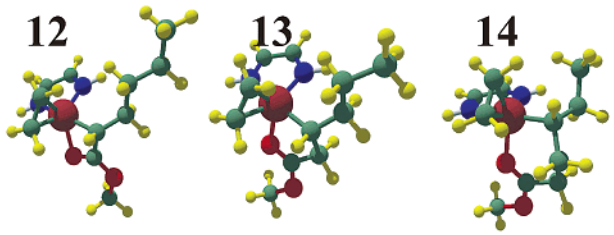

Figure 2. Optimized structures of the most stable isomers of the ethylene π-complexes derived from the four-, five-, and six-membered chelates (Ni-catalyst).

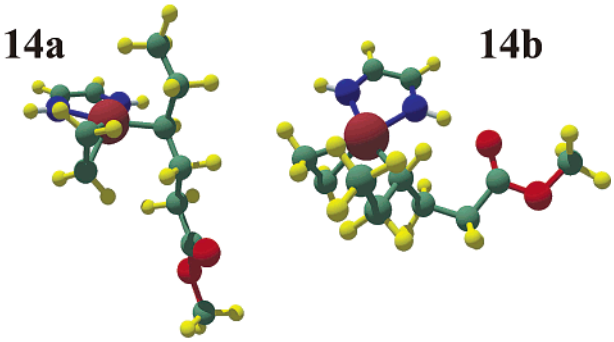

Figure 3. Examples of the alternative structures of the ethylene π-complexes (without the chelating Ni−O bond).

for the Ni-systems are much lower (−10.7, −8.1, and −7.7 for the four-, five-, and six-membered chelate, respectively) than those obtained for the π-complexes formed from the alkyl complexes (−18.8 kcal/mol). The same is true for the acrylate π-complexes of nickel. Unlike in the case of the alkyl-acrylate complexes, the π-binding mode is strongly preferred (by ca. 3−5 kcal/mol, see Table 2) in the acrylate complexes derived from the chelates. This can be attributed to a repulsive interaction between the chelate oxygen and the carbonyl oxygen of acrylate, destabilizing the O-complexes.

In a previous study[20] we have shown for the Pd-catalyst that besides the chelated structures there exist a large number of higher energy isomers of **12**, **13**, and **14** in which the chelating Pd−O bond has been broken. This is also the case for the Ni-catalyst. All the structures without the Ni−O chelating bond are higher in energy compared to the most stable, chelated structures (Figure 2). In Figure 3 two examples of such isomers are presented; they are analogous to the structures discussed previously for the Pd-catalyst. The complexes **14a** and **14b** are higher in energy then **14** by 16.9 and 6.3 kcal/mol, respectively. The corresponding Pd-complexes were found to be higher in energy than the most stable isomer by 11.8 and 1.7 kcal/mol, respectively. Thus, the energy differences between the analogous chelated and nonchelated structures are larger for Ni than for Pd by ca. 5 kcal/mol. This difference can be attributed to an increased stability of the Ni-chelates compared to Pd (see Figure 1), reflecting the higher oxophilicity of the Ni-systems.

As a next step, we have performed unconstrained MD simulations (at 300 and 1300 K) for the Pd- and Ni-complexes **14a** and **14b** in order to check the free energy stability of the nonchelated complexes at higher temperatures. The results show that for both metals the geometries oscillate in the vicinity of the corresponding local minima. No spontaneous isomerization toward

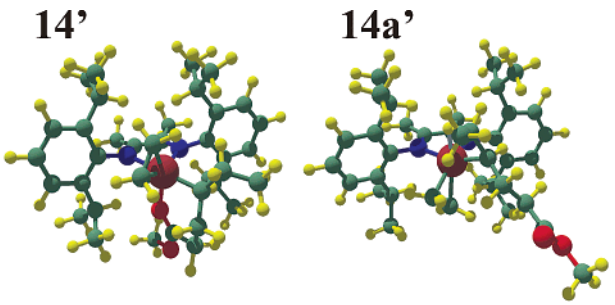

Figure 4. Lowest energy isomer of **14′** (chelated) and an example of the higher energy complex without chelating bond (**14′b**) calculated for the real catalyst.

chelated structures has been observed, nor toward any other isomers. Thus, it can be concluded that the nonchelated isomers are stable on their free energy surfaces. They are in addition separated from other isomers by barriers larger than 2.5 kcal/mol.

Further, the opening of the six-membered chelate prior to ethylene insertion was studied by a slow-growth MD simulation for Ni and Pd ethylene-chelate complexes **14**. The metal−oxygen distance has been used as a reaction coordinate, increasing from the values in **14** (2.29 Å for Pd and 2.08 Å for Ni) up to 4.23 Å (8 bohr). The TS regions were located at a M−O distance of 3.12 and 3.71 Å for Ni and Pd, respectively. The activation energies and free energies are as follows: $\Delta E^{\ddagger} = 6.8$ kcal/mol, $\Delta G^{\ddagger} = 11.3$ kcal/mol for Pd, and $\Delta E^{\ddagger} = 10.9$ kcal/mol, $\Delta G^{\ddagger} = 14.4$ kcal/mol for the Ni-catalyst. Thus, for the Pd-catalyst the activation barrier has been found to be lower than for the Ni-complex.

The results presented above have been obtained for the generic catalyst, in which the presence of the bulky substituents is neglected. It might be expected that the steric bulk would facilitate the chelate opening, since the chelating oxygen occupies an axial position and must interact strongly with the catalyst substituents. To investigate the steric effect, calculations have been carried out for the complexes **14′** and **14a′** with the real Ni- and Pd-diimine catalysts (analogous to **14** and **14a**). As an example, the optimized geometries of **14′** and **14a′** with the Ni-catalyst are presented in Figure 4. The results show that, indeed, the energy difference between **14′** and **14a′** is strongly decreased compared to the model systems (**14**, **14a**) for both the Ni- and Pd-complexes. The opened-chelate complex **14a′** is higher in energy than **14′** by 4.2 and 7.5 kcal/mol, for the Ni- and Pd-catalyst, respectively. Thus, for the real systems the endothermicity of the chelate opening prior to insertion, **14′** → **14a′**, is decreased compared to the generic systems by 12.7 and 4.3 kcal/mol for the Ni- and Pd-system, respectively. This effect appears as a result of a strong destabilization of the chelated systems in the congested geometries of **14′**. The systems without additional chelating bonds, **14a′**, are only slightly influenced by the bulky substituents on the catalyst. It is not surprising that the effect of the steric bulk is substantially larger for Ni than for Pd, as all the bonds involving Ni are typically shorter than those containing Pd by 0.1−0.2 Å, and thus, the nickel systems are more congested. These results clearly demonstrate that the steric bulk in real systems facilitates the chelate opening.

Table 3. Ethylene Insertion Barriers after the Acrylate Insertion (from MD simulations)

	activation barriers[a]			
	Ni-catalyst		Pd-catalyst	
initial complex	$\Delta E^{\ddagger}$	$\Delta G^{\ddagger}$	$\Delta E^{\ddagger}$	$\Delta G^{\ddagger}$
four-membered chelate:				
12	28.07	32.87	35.79	38.23
five-membered chelate:				
13	33.91	36.51	41.20	44.74
six-membered chelate:				
14	38.78	40.81	49.89	53.36
14c	18.79	20.41	23.97	30.37

[a] In kcal/mol.

Ethylene Insertion Starting from the Chelate-Ethylene Complexes. The activation barriers for the ethylene insertion starting from the chelate-ethylene complexes are presented in Table 3; these results have been obtained from the slow-growth MD simulations, with the distance between the α-carbon of the chain and an olefin carbon chosen as a reaction coordinate. The results clearly show that in each case the barriers are substantially lower for the Ni- than for the Pd-catalyst. For all the systems, the ethylene insertion reactions starting from the most stable chelate structures **12**, **13**, and **14** have very high barriers (38−53 and 32−41 kcal/mol for Pd and Ni, respectively), much higher than the ethylene insertion barriers into the metal−alkyl bond ($\Delta E^{\ddagger} = 16.8$ and 14.2 kcal/mol for Ni and Pd, respectively). These results demonstrate that the ethylene insertion cannot proceed from the most stable ethylene-chelate structure.

Let us now discuss the trajectories obtained from the simulations in more detail. In the following we will discuss only the trajectories for the six-membered chelate. The results obtained for the five- and four-membered chelates are qualitatively similar. The examples of the structures observed for the insertions starting from the six-membered chelates (**14**) are shown in Figure 5, together with the metal−oxygen and the metal−γ-hydrogen distances along the MD trajectories. For both metals, the chelating bond is practically present along the whole insertion pathway. The Ni−O and Pd−O bonds are weakened after passing the TS region; they are extended by 0.07 and 0.35 Å compared to the initial structures, respectively. In both cases, the insertion leads directly to the eight-membered chelate, as reflected by the Ni−O and Pd−O bond shortening after passing the TS. For both Ni- and Pd-catalysts there is practically no interaction between the metal and the γ-hydrogen (i.e., α-hydrogen in the initial structure); the distance between the metal atom and the γ-hydrogen increases as the insertion proceeds. This is different from the usual olefin insertions observed in the homopolymerization reactions, where the TS is usually stabilized by a γ-hydrogen interacting with the metal. It seems very likely that the lack of this γ-hydrogen stabilization is responsible for the very high insertion barriers observed here. In the most stable structures of **14**, **15**, and **16** the α-hydrogen of the $-CH(R^1)(R^2)$-$COOCH_3$ group (i.e., the γ-hydrogen of the product) points toward ethylene (see Figures 2 and 6), and during the insertion pathways the $-CHR^1R^2$ group rotates in a direction that increases the metal−hydrogen distance. Therefore, we also performed simulations for the alter-

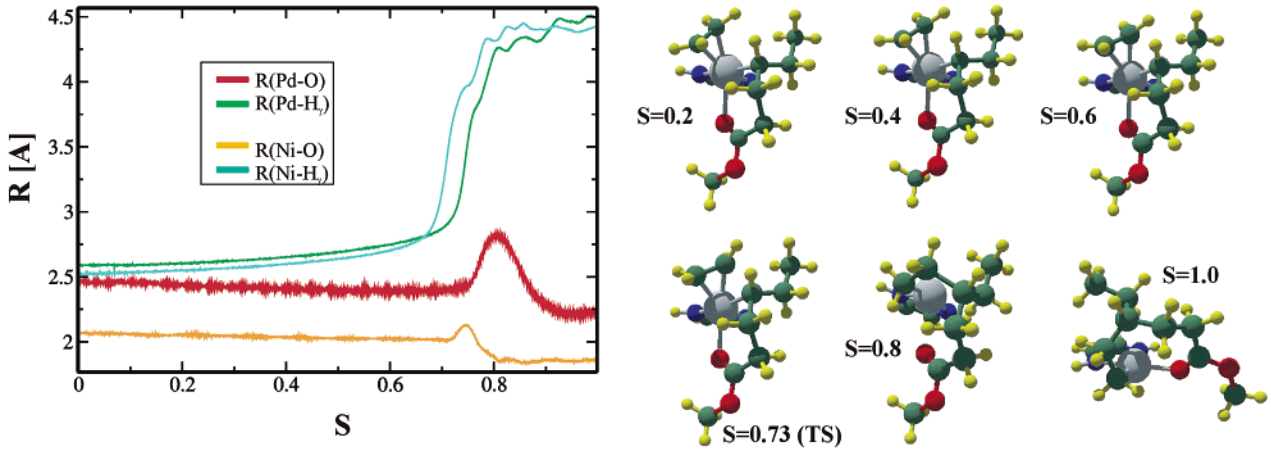

Figure 5. Changes in the interatomic distances for M−O (carbonyl) and M−H$_\gamma$ (M = Ni, Pd) along the MD trajectory obtained from the ethylene insertion starting from complex **14** (see Scheme 1) [left] and examples of the structures from the simulations [right]; *S* denotes a reaction progress variable.

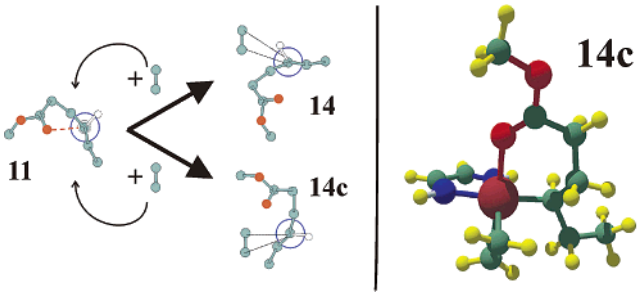

Figure 6. Schematic representation of formation of the alternative chelate-ethylene complexes **14** and **14c** from the chelate **11** [left] together with the optimized structure of **14c** [right].

native isomers of **14**, in which the hydrogen is located "on the opposite side" of ethylene (see Figure 6). In the insertion reaction starting from such a structure **14c**, the γ-hydrogen interaction along the pathway is possible. However, complex **14c** is higher in energy compared to **14** by 4.1 and 5.1 kcal/mol for Pd and Ni, respectively.

Figure 7 displays the metal−oxygen and metal−γ-hydrogen distances along the trajectories for the insertions starting from the Ni- and Pd-complexes **14c**. The insertion barriers are listed in Table 3. The activation barriers for the insertion starting from **14c** are substantially lower than those obtained for **14**. However, for both metals they are still noticeably higher than the activation barriers for olefin insertion observed in the homopolymerization processes.

The curves of Figure 7 show that, indeed, during the reaction the γ-hydrogen approaches the metal, and in the TS region the Pd−H$_\gamma$ and Ni−H$_\gamma$ distances are typical for γ-agostic interactions (1.93 and 1.81 Å for Pd and Ni, respectively). Together with the fact that the insertion barriers are much lower than those discussed previously, this result emphasizes the role of the γ-agostic interactions in the olefin insertion reactions. However, the system spontaneously evolves toward an eight-membered chelate for both metals after passing the TS. This is reflected in a decrease in the metal−oxygen distances. It should be pointed out here that the chelating metal−oxygen bond is present along the whole pathway also in the case of insertions starting from **14c**. In the TS region the metal−oxygen distance is extended only by 0.16 and 0.22 Å for Ni and Pd, respectively. The conclusions reached here from our finite temperature MD calculations differ from those obtained previously[20] from static DFT calculations where the chelating bond breaks before reaching the insertion TS. This demonstrates that the MD approach is especially valuable for studying reactions for which there exist a large number of isomeric structures, giving rise to many alternative pathways with different isomeric TS geometries.

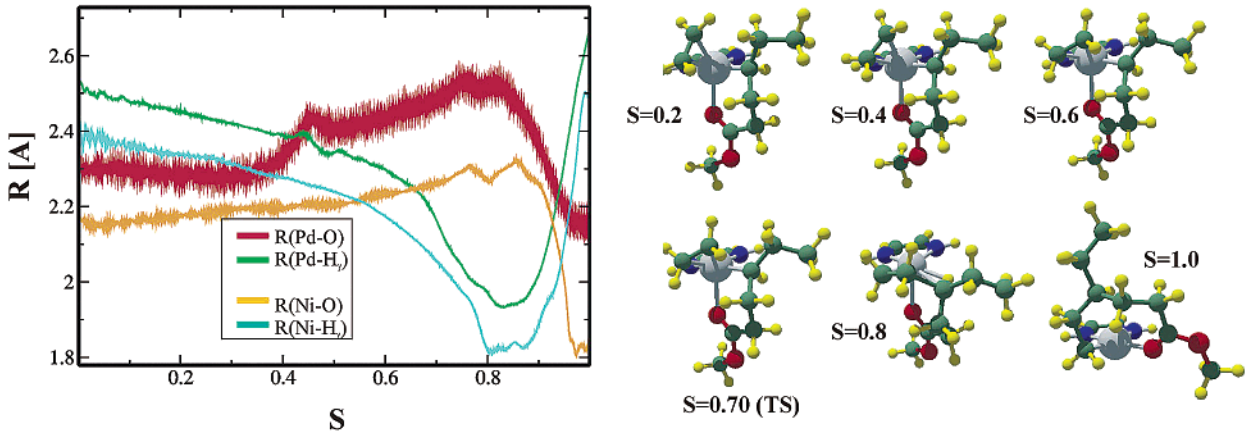

Figure 7. The same as in Figure 5 for the ethylene insertion starting from complex **14c**.

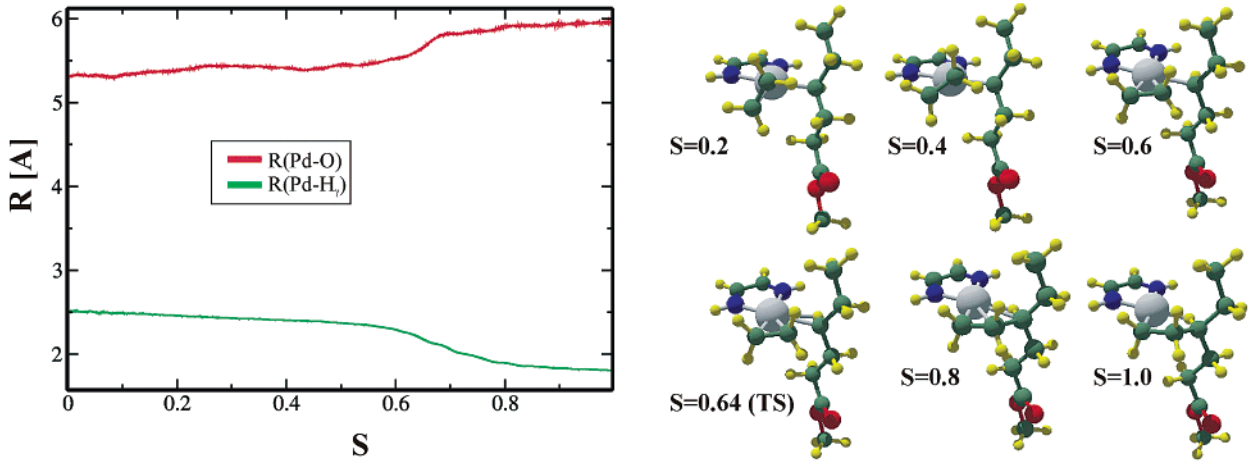

Figure 8. The same as in Figure 5 for the ethylene insertion starting from complex **14a**.

Finally, for the Pd-catalyst we would like to discuss the MD results for yet another ethylene insertion pathway, starting form the higher energy complex **14a**, in which the chelating Pd−O bond has been broken. In the previous paper we suggested the two-step chelate opening mechanism (see Scheme 1c), in which the chelating bond is broken at the π-complex stage, i.e., prior to the ethylene insertion. The static DFT calculations have demonstrated that the barriers for insertion starting from π-complexes without chelating M−O bonds are comparable to the barriers of ethylene insertion in the homopolymerization processes. Further, the oxygen atom practically does not play a role in the insertion involving π-complexes without chelating M−O bonds. Here, we have performed MD simulation for the insertion involving π-complexes without chelating M−O bonds, to check whether the same is true at the free energy surface when higher temperatures are taken into account. Figure 8 shows the Pd−O and Pd−H_γ distances along the MD trajectory, and the activation barriers are listed in Table 3. The results demonstrate that at T = 300 K the insertion proceeds according to the mechanism typical for ethylene homopolymerization. The distance between the metal and the γ-hydrogen decreases along the pathway, and the insertion product is a γ-agostic complex. The presence of carbonyl oxygen does not influence the reaction; it stays remote (5.3−6 Å). The calculated activation barrier [$\Delta E^{\ddagger}$ = 17.1 kcal/mol, $\Delta G^{\ddagger}$ = 19.1 kcal/mol] for the insertion is comparable with the homopolymerization activation barriers. Very similar results were obtained for the insertion starting from **14b**: $\Delta E^{\ddagger}$ = 17.02 kcal/mol, $\Delta G^{\ddagger}$ = 22.3 kcal/mol.

The results presented here clearly demonstrate that the insertions starting from the higher energy isomers of the ethylene-chelate complexes in which the chelating bond has been broken have much smaller activation barriers, comparable to those observed in ethylene homopolymerization. This, however, does not explain the differences in the copolymerization activity of Pd- and Ni-diimine complexes, as the barriers for the ethylene insertion into the Ni−alkyl bond are smaller (14.2 kcal/mol) than those for the Pd−alkyl bond (16.8 kcal/mol). Thus, it may be concluded that the ethylene insertion following the insertion of the polar monomer is not a crucial factor for the copolymerization activity. It is the initial poisoning of the catalyst by formation of the O-complexes and the chelate opening prior to the ethylene insertion that seems to be responsible for differences in catalytic activity of the Ni- and Pd-diimine complexes.

Concluding Remarks

We have carried out a study in which we compare Pd- and Ni-diimine complexes as acrylate/ethylene copolymerization catalysts. The main goal was to understand the differences between the Pd- (active copolymerization catalyst) and Ni-systems (inactive in polar copolymerizatation under the same conditions). We have demonstrated that the acrylate insertion follows the same mechanism for the Ni- and Pd-complexes. For the real diimine catalyst, the insertion of the methyl acrylate into the metal−alkyl bond has a slightly higher barrier for the Ni- (13.5 kcal/mol) than for the Pd-catalyst (12.4 kcal/mol).[20] In both cases, however, the activation barriers for the acrylate insertion are lower than the ethylene insertion barriers (16.8 and 14.2 kcal/mol for Pd- and Ni-catalyst, respectively). Thus, the acrylate insertion barriers do not explain the difference in the catalytic activity of the Pd- and Ni-complexes.

The acrylate insertion leads to the formation of a chelate complex with an oxygen atom bound to the metal. Further insertion of ethylene into the M−C bond starting from the chelate must follow a multistep process. The first step involves π-complexation of ethylene to the metal center of the chelate followed by opening of the chelate (M−O bond breaking) and subsequent insertion of ethylene into the M−C bond. For the generic catalyst [Ar = H, R = H] the endothermicity of such a chelate opening prior to the insertion is higher for Ni- than for the Pd-system (by ca. 5 kcal/mol); so is its activation barrier (by ca. 3 kcal/mol). However, the steric bulk on the catalyst facilitates the chelate opening, and this effect is stronger for nickel than for palladium. We have found that for the real catalysts [Ar = 2,6-C_6H_3(i-Pr)$_2$; R = CH_3] the endothermicity of the chelate opening reaction is decreased compared to the generic systems by ca. 12.7 and 4.3 kcal/mol for the Ni- and Pd-system, respectively. It is thus clear that for the real systems with bulky substituents the chelate opening reactions are not responsible for the differences in catalytic activity between the Ni and Pd.

The present results suggest that the most important difference between Pd- and Ni-diimine complexes as catalysts for methyl acrylate/ethylene copolymerization is the fact that the Ni-catalyst initially is poisoned by O-binding of methyl acrylate to the metal center. For the Ni-catalyst the O-binding mode is energetically preferred by ca. 3 kcal/mol, while for the Pd-system the π-complex has the lower energy.[19] Thus, it may be concluded that the use of bulky catalysts with a less oxophilic character (i.e., neutral systems) should be promising in polar copolymerization.

Our results have further revealed a new role for steric bulk in polar copolymerization processes. Thus, steric bulk is seen to weaken chelate bonds between the metal center and the polar group that might otherwise poison the catalyst. Understanding this role should be helpful in the design of new catalysts.

Acknowledgment. This work has been supported by the National Sciences and Engineering Research Council of Canada (NSERC) as well as donors of the Petroleum Research Fund, administered by the American Chemical Society (ACS-PRF No. 36543-AC3). T.Z. acknowledges a Canada Research Chair from the Canadian government. A.M. acknowledges a NATO Postdoctoral Fellowship. Important parts of the calculations have been performed on the UofC MACI cluster.

OM021044E